



Published in final edited form as:

Nature. 2013 May 9; 497(7448): 263–267. doi:10.1038/nature12135.

Phosphatidylserine receptor BAI1 and apoptotic cells as new promoters of myoblast fusion

Amelia E. Hochreiter-Hufford^{1,2,3}, Chang Sup Lee^{1,2,3}, Jason M. Kinchen^{1,2,3}, Jennifer D. Sokolowski^{3,6}, Sanja Arandjelovic^{1,2,3}, Jarrod A. Call^{4,5}, Alexander L. Klibanov^{4,5}, Zhen Yan^{4,5}, James W. Mandell^{3,6}, and Kodi S. Ravichandran^{1,2,3}

¹Department of Microbiology, Immunology and Cancer Biology, University of Virginia, Charlottesville, Virginia 22908, USA

²Beirne B. Carter Immunology Center, University of Virginia, Charlottesville, Virginia 22908, USA

³Center for Cell Clearance, University of Virginia, Charlottesville, Virginia 22908, USA

⁴Robert M. Berne Cardiovascular Research Center, University of Virginia, Charlottesville, Virginia 22908, USA

⁵Department of Medicine, University of Virginia, Charlottesville, Virginia 22908, USA

⁶Department of Pathology, University of Virginia, Charlottesville, Virginia 22908, USA

Abstract

Skeletal muscle arises from the fusion of precursor myoblasts into multinucleated myofibers^{1,2}. While conserved transcription factors and signaling proteins involved in myogenesis have been identified, upstream regulators are less well understood. Here, we report an unexpected discovery that the membrane protein BAI1, previously linked to recognition of apoptotic cells by phagocytes³, promotes myoblast fusion. Endogenous BAI1 expression increased during myoblast fusion, and BAI1 overexpression enhanced myoblast fusion via signaling through ELMO/Dock180/Rac1 proteins⁴. During myoblast fusion, a fraction of myoblasts underwent apoptosis and exposed phosphatidylserine (PtdSer), an established ligand for BAI1³. Blocking apoptosis potently impaired myoblast fusion, and adding back apoptotic myoblasts restored fusion. Furthermore, primary human myoblasts could be induced to form myotubes by adding apoptotic myoblasts, even under normal growth conditions. *In vivo*, myofibers from *Bai1*^{-/-} mice are smaller than wild-type littermates. Muscle regeneration after injury was also impaired in *Bai1*^{-/-} mice, highlighting a role for BAI1 in mammalian myogenesis. Collectively, these data identify signaling via the phosphatidylserine receptor BAI1 and apoptotic cells as novel promoters of myoblast fusion, with significant implications for muscle development and repair.

Users may view, print, copy, download and text and data-mine the content in such documents, for the purposes of academic research, subject always to the full Conditions of use: http://www.nature.com/authors/editorial_policies/license.html#terms

Author Contributions: A.E.H. designed, performed and analyzed most of the experiments in this study with input from K.S.R. C.S.L. generated and supplied the *Bai1*^{-/-} mice, and provided GST-tagged BAI1 TSR. J.M.K. assisted with time-lapse and shRNA studies, and myofiber cross-sectional area analyses. S.A. helped with the *in vivo* muscle regeneration and *ex vivo* primary myoblast cultures. J.D.S. processed, stained and analyzed the mouse embryonic tissues. A.K. provided PtdSer liposomes for these studies. J.A.C. and Z.Y. assisted with the cardiotoxin injury model. J.W.M. provided intellectual input on the *in vivo* BAI1 studies. A.E.H. and K.S.R. wrote the manuscript with comments from co-authors.

Mammalian skeletal muscle is formed by the proliferation, differentiation and fusion of myogenic precursor cells (myoblasts) into multinucleated myofibers. The Dock180 protein⁵ and its partner ELMO⁴ function as guanine nucleotide exchange factor to activate the GTPase Rac⁶ and all three have been linked to myoblast fusion⁷⁻¹². The 7-transmembrane protein BAI1 (a member of the adhesion-type GPCR family) mediates recognition of PtdSer on apoptotic cells (Fig. 1a), and signals through the ELMO/Dock180/Rac1 pathway³. We asked whether BAI1 might also play a role in myoblast fusion.

We readily detected endogenous BAI1 expression in developing embryonic day E14.5 mouse myofibers (Fig. 1b). Shifting mouse C2C12 myoblasts from growth medium (GM) to low-serum fusion medium (FM), induces formation of multinucleated, myosin-expressing myotubes¹³, and provides a quantifiable in vitro model of myogenesis^{14,15}. While BAI1 was expressed in undifferentiated C2C12 myoblasts, a reproducible 4-fold increase in BAI1 protein was observed in fusing cultures (Fig. 1c). Since siRNA mediated knockdown of BAI1 in C2C12 myoblasts was variable and inefficient, we asked whether BAI1 overexpression could provide a 'gain of function'. C2C12 myoblast clones stably overexpressing BAI1-GFP protein showed enhanced myoblast fusion (Fig. 1d and 1e), and the increased fusion was seen with multiple independent BAI1-GFP clones. Lentivirus-based overexpression of BAI1 in C2C12 cells (maintained as heterogeneous populations) also displayed greater fusion with 73% increase in the fusion index (the fraction of total nuclei that are contained within the fused myotubes, see methods) ($P < 0.001$; Fig. 1h). Moreover, myotubes in cultures overexpressing BAI1 appeared longer with more nuclei compared to control cultures. Counting the number of myotubes with 2-4 nuclei (small myotubes) and ≥ 5 (large myotubes) confirmed that BAI1 overexpression increases the total number of myotubes and the number of nuclei per myotube ($P < 0.01$; Fig. 1h).

We next asked whether BAI1-mediated C2C12 fusion was dependent on the ELMO/Dock180/Rac1 signaling module³. C2C12 myoblasts with knockdown of ELMO2 (the predominant isoform in myoblasts; Fig. 1f), formed fewer myotubes and were reduced in size and nuclei content (Fig. 1g). To test the requirement for ELMO in BAI1-mediated enhanced fusion, we transduced a BAI1 mutant (BAI1-AAA) unable to engage the ELMO/Dock180/Rac1 module³. BAI1-AAA overexpression did not increase the fusion index, total number of myotubes or nuclei per myotube (Fig. 1h). The fusion-promoting effect of BAI1 also depends on Rac activity, as the Rac inhibitor EHT1864¹⁶ effectively inhibited myoblast fusion in BAI1 overexpressing cells ($P < 0.01$, $P < 0.001$; Fig. 1i). These data suggest that the membrane protein BAI1, signaling via the ELMO/Dock180/Rac1 module, can enhance mammalian myoblast fusion.

During phagocytosis, BAI1 on phagocytes recognizes PtdSer, a near-universal marker exposed on the surface of apoptotic cells; previous studies have suggested that transient externalization of PtdSer is necessary for myoblast fusion^{17,18}. Myoblast fusion was strikingly inhibited by masking PtdSer in fusing cultures, using either PtdSer-binding domain of BAI1 (GST-TSR)³ or a commercially available PtdSer-specific antibody fragment (Supplementary Fig. 1a and b). Interestingly, we also found that a significant fraction of C2C12 myoblasts underwent cell death within 24 hours after switching to fusion medium (associated with rounding up and detachment from the plate). Such cells displayed

several known features of apoptosis, with 17% of cells positive for annexin V, 9% positive for TO-PRO-3 (which enters apoptotic cells via caspase-activated channels¹⁹), and 9% positive for active caspase-3 ($P<0.01$, $P<0.05$; Fig. 2a). These may be an underestimation due to the unavoidable loss of apoptotic cells during staining protocols. We also analyzed paraspinal muscle tissue at different stages of embryogenesis, and could readily detect apoptotic cells labeled with cleaved caspase 3 (73.8 ± 32.0 per mm^2) that were in contact with E14.5 myofibers (Fig. 2b, left panel). Several of these apoptotic cells also displayed blebbing (Fig. 2b, right panel). Of note, E14.5 is also the stage when we observed a strong BAI1 staining of developing myofibers (Fig. 1b).

We next tested whether apoptosis was required for myoblast fusion. Adding z-VAD-FMK (zVAD), a pan-caspase inhibitor that blocks apoptosis, potently inhibited myoblast fusion (51% decrease in fusion index, $P=0.0002$; Fig. 2c). Similar results were observed with another pan-caspase inhibitor, Q-VD-OPH (Q-VD). Supplementing insulin-transferrin-selenium (ITS) to fusion medium enhances myoblast fusion, yielding large, sheet-like myotubes within 24–48 hours (Supplementary Fig. 1c). Caspase inhibition also potently inhibited ITS-enhanced fusion (67% decrease, $P<0.0001$; Supplementary Fig. 1c). zVAD blocked fusion of BAI1-GFP overexpressing cells, suggesting that the fusion-promoting effect of BAI1 also depends on cell death within fusing cultures (Fig. 2d).

Concerns that the caspase inhibitor-mediated block of myoblast fusion could have arisen due to an unintended, non-specific effects were overcome when the removal of zVAD from myoblast cultures, even after treatment for 5 days, re-initiated fusion (data not shown). Moreover, zVAD inhibition of myoblast fusion depended on the time when the myoblasts were exposed to the drug; zVAD was far less effective when added to C2C12 cells already switched to fusion medium and after the appearance of floating/apoptotic cells (Fig. 2e). These observations suggest that the emergence of apoptotic myoblasts in fusing cultures is essential for normal myoblast fusion.

Myogenin (MyoG) is an essential basic-helix-loop-helix myogenic transcription factor involved in the development of skeletal muscle *in vivo*²⁰. Caspase inhibition did not block the approximate 60-fold upregulation of the *MyoG* transcript (Supplementary Fig. 2), even though both zVAD and Q-VD effectively blocked expression of myosin, another well-known differentiation marker (Fig. 2c and Supplementary Fig. 1c). This suggests that caspase inhibition does not block all differentiation steps, and that caspase-mediated apoptosis during myoblast fusion is required either downstream or parallel to MyoG.

We next asked whether adding apoptotic myoblasts could ‘rescue’ fusion in zVAD-treated cultures. We collected the floating/apoptotic myoblasts from fusing cultures without zVAD, gently resuspended them in fresh fusion medium containing zVAD, and added them to zVAD-treated fusing cultures (see schematic in Fig. 3a). Adding apoptotic myoblasts effectively rescued zVAD-inhibited myoblast fusion, with a 149% increase in the fusion index ($P<0.01$; Fig. 3b). The added myoblasts exposed phosphatidylserine (Supplementary Fig. 3a), but did not attach to the tissue culture plate, or fuse on their own (Supplementary Fig. 3b); thus, the simple increase in cell density or adherence could not explain the fusion-promoting effect. Importantly, supernatants from fusing myoblast cultures (passed through a

0.2µm filters) failed to rescue zVAD-inhibited fusion (Fig. 3b). Adding one apoptotic myoblast per two viable myoblasts could maximally rescue the zVAD-inhibited fusion (Supplementary Fig. 3c), while adding too many dying myoblasts was less effective.

Consistent with the observation that PtdSer exposure is necessary for myoblast fusion, masking PtdSer on apoptotic myoblasts (with GST-TSR³) failed to rescue fusion ($P<0.001$; Supplementary Fig. 3d). When we tested whether apoptotic myoblasts delivered a unique signal or if any apoptotic cell-type could stimulate fusion, apoptotic primary mouse thymocytes also rescued zVAD-inhibited myoblast fusion ($P<0.001$; Supplementary Fig. 4c). These data further suggested caspase inhibition itself does not have a non-specific effect, and that myoblasts can fuse in the presence of zVAD if supplied apoptotic cells. Collectively, these observations suggest that apoptotic myoblasts are necessary to promote myoblast fusion, requiring PtdSer-dependent cell-cell contact between apoptotic and viable myoblasts.

Normally, fusion is deficient or absent in C2C12 myoblasts cultured in growth medium (Fig. 3c). Strikingly, adding apoptotic myoblasts to the myoblast cultures in growth medium stimulated fusion, (70% increase in fusion index, $P<0.05$; Fig. 3c). This effect of apoptotic myoblasts was again dependent on phosphatidylserine exposure (Fig. 3c). Since myoblasts in growth medium continue to divide with no apparent cell death, these cultures had more nuclei at the end of the assay, artificially lowering the fusion index values. However, counting the number of myotubes containing 2-4 nuclei (small myotubes) and ≥ 5 nuclei (large myotubes) revealed that apoptotic myoblasts significantly promoted myotubes with ≥ 5 nuclei $P<0.001$; Fig. 3c). This fusion promoting effect of apoptotic cells in growth medium was not caused by lowering nutrients in the culture medium (mimicking low mitogen fusion medium conditions); adding 'viable' T lymphocytes, which proliferated and consumed nutrients from the culture medium did not promote fusion, while apoptotic lymphocytes triggered fusion ($P<0.001$, $P<0.01$; Supplementary Fig. 4b). We then asked the applicability of these observations to primary human myoblasts. Primary human myoblasts readily fused and formed myotubes when cultured in fusion medium but not in growth medium (Fig. 3d, left image). Adding apoptotic C2C12 myoblasts stimulated fusion of primary human myoblasts in growth medium, with 170% increase in fusion index ($P<0.05$; Fig. 3d). Thus, dying cells could stimulate mouse and human myoblasts to fuse and form myotubes.

To address the function of BAI1 in myoblast fusion *in vivo*, we generated *Bai1*^{-/-} mice using embryonic stem (ES) cells with an exon trap mutation of exon 2. We compared myofibers from the tibialis anterior (TA) muscle of 12-week old male *Bai1*^{+/+} versus *Bai1*^{-/-} littermate mice (Fig. 4a). While *Bai1*^{-/-} muscles did contain fully formed myofibers, they contained smaller-sized fibers as well as clusters of very small fibers (Fig. 4b, arrowheads). We took an unbiased approach to quantitate the cross-sectional areas (CSA) of each myofiber using the Cell Profiler software tool²¹, and plotted the frequency distribution of the myofibers (Fig. 4c). The TA muscles of the *Bai1*^{-/-} mice were skewed towards smaller myofibers compared to control littermates. Classifying the myofibers as either small (<1500 µm²) or large (>1500 µm²), the *Bai1*^{-/-} TA muscle had a greater proportion of small myofibers and significantly fewer large myofibers, suggesting a need for

Bai1 in larger myofiber formation ($P < 0.05$, $n = 5-8$ mice; Fig. 4c, right panel). Additionally, the average myofiber CSA of *Bai1*^{-/-} mice (per mouse) was again significantly reduced compared to *Bai1*^{+/+} littermates ($P < 0.05$, $n = 5-8$ mice; Fig. 4d). It is notable that *Bai1*^{-/-} mice did develop major skeletal muscle tissues, possibly due to the continued expression of the *Bai1* homologues *Bai2* and *Bai3* ($P < 0.05$, $n = 5$ mice per genotype; Supplementary Fig. 5a). These data suggested a requirement for BAI1 in optimal myofiber development *in vivo*.

To test whether BAI1 might influence muscle repair and regeneration, we used the cardiotoxin (cdx)-induced muscle injury and repair model²² (Supplementary Fig. 5b). After cardiotoxin injection into TA muscles of control and *Bai1*-null mice, we analyzed regenerating fibers after 14 days (shown in images of Fig. 4e). Focusing our analysis on the regenerated fibers, the average myofiber cross sectional areas of the *Bai1*^{-/-} mice were reduced compared to the *Bai1*^{+/+} littermates ($P < 0.05$, $n = 3$ mice; Fig. 4f and Supplementary Fig. 5c). Using centralized nuclei number per myofiber to calculate the *in vivo* fusion index (see methods²³), the *Bai1*^{-/-} mice displayed a 31% reduction compared to littermate controls ($P < 0.01$, $n = 6-8$ mice; Fig. 4e, right). These results demonstrated a requirement for BAI1 in the optimal fusion and regeneration of myofibers after muscle injury.

Since BAI1 is a phagocytic receptor for apoptotic cells³ and apoptotic cells influence myoblast fusion, an interesting possibility was that engulfment of dying myoblasts by healthy myoblasts contributed to myoblast fusion. Alternatively, engagement by the dying myoblasts of the healthy myoblasts might have provided signaling cues (not contingent on phagocytosis) that contributed to fusion. We found that the healthy myoblasts could engulf apoptotic myoblasts *in vitro*, an observation not reported previously (Fig. 4g). We next used time-lapse microscopy to investigate the fate of apoptotic myoblasts emerging during fusion and what might happen to the nuclei of apoptotic cells (although nuclei of apoptotic cells are damaged and unlikely to directly contribute to the multi-nucleated myotubes). The apoptotic myoblasts, which were labeled by adding the viability dye TO-PRO-3 to the fusing medium, appeared to not be engulfed by nascent myotubes; rather, TO-PRO-3 stained cells remained in close contact with the newly forming myotubes (Fig. 4h, Supplementary Fig. 6 and Supplementary Movie SM1). This close association (without obvious phagocytosis) was confirmed with a second viability dye eFlour; 62% of dying myoblasts were in close proximity (but not within) myosin-positive myotubes, and 94% of myotubes were in close proximity to dying myoblasts (Fig. 4i). However, these data do not rule out additional roles for phagocytosis during myoblast fusion (perhaps for acquiring energy). Interestingly, we could detect actin polymerization at some of the contacts between apoptotic cells and fusing myotubes (Supplementary Fig. 7).

The data presented in this report identify a novel and unexpected positive role for the PtdSer receptor BAI1 in promoting fusion of skeletal myoblasts to form myotubes. Lowered expression of *Bai1* was seen in transcriptome analyses of muscles from Duchenne Muscular Dystrophy patients²⁴. Additionally, expression levels of the genes that encode ELMO2 and Dock180 are altered in skeletal muscle disorders²⁴⁻²⁷. Thus, identification of BAI1 as a novel promoter of myoblast fusion, and the link between ELMO/Dock180/Rac1 signaling pathway and myoblast fusion⁷⁻¹² has relevance for mammalian skeletal muscle development and muscle disorders.

These data also identify the interaction between apoptotic and healthy myoblasts as a new type of fusion cue that in turn promotes fusion between healthy myoblasts. Apoptotic cells appear to contact the viable fusing myoblasts/myotubes without fusing with them, suggesting an interaction distinct from the one between a fusion competent myoblast and a founder cell seen in *Drosophila*^{1,28}. Since cell death is often associated with weight training and strength conditioning exercises that promote muscle mass²⁹, further studies targeting the triggering of BAI1 or other PtdSer receptors in stimulating muscle growth could be beneficial for promoting recovery after injuries.

While apoptosis and cell clearance have been studied for many years, dying cells are generally considered a nuisance that need to be removed quickly. The concept that the body may use cell death not only to rid itself of unwanted cells, but also to use them to beneficially regulate differentiation adds an important dimension to considering cell turnover within tissues and organisms. Activated lymphocytes and other cell types are known to transiently expose phosphatidylserine in non-apoptotic contexts³⁰. An intriguing possibility is that these transient PtdSer exposures, via cell-cell contact (e.g. in germinal centers of lymph nodes during immune responses), might be involved in differentiation events in other tissues.

Methods

Cell culture and myoblast fusion assay

C2C12 murine skeletal muscle myoblasts (American Type Culture collection) were maintained at sub-confluent densities in growth medium (DMEM supplemented with 20% heat-inactivated FBS) at 8.5% CO₂ 37°C. Normal human primary skeletal muscle myoblasts (HSMM; Clonetics) were maintained at sub-confluent densities in defined SkGM-2 medium (Clonetics) at 5% CO₂ 37°C. Myoblast fusion (of both C2C12 and primary human myoblasts) was induced by rinsing 70-80% confluent cultures once with PBS and switching them to fusion medium (DMEM supplemented with 2% heat-inactivated horse serum). Fusion medium was replaced every 24 hours for a total of 72 hours, unless specified otherwise. Where indicated, zVAD-fmk (100 µM; Enzo Life Sciences), Q-VD-OPH (100-150 µM; SM Biochemicals), Dead-Cert imab6 fragment (100 µg/mL; Immunosolv), or GST-tagged BAI1 TSR (100 µg/mL)³ was added to cultures 24 hours before switching to fusion medium and maintained throughout the experiment. Where indicated, EHT 1864 (10 µM; Sigma-Aldrich) or Insulin-Transferrin-Selenium (1X; Gibco) was added at the same time as fusion medium and maintained throughout the experiment.

Fluorescence microscopy and quantitative analysis of fusion

To measure fusion, myoblasts were plated in growth medium on 2-chamber LabTek II Permanox chamber slides (Nunc) at 1×10⁵ cells/well (C2C12) or 7.5×10⁴ cells/well (HSMM and C2C12 in GM add-back experiments). Myoblasts were induced to undergo myogenic differentiation as described above. Myoblasts/myotubes were washed and fixed with 4% paraformaldehyde in PBS for 20 min at room temperature and permeabilized in 0.2% Triton X-100, 0.1% citrate in PBS for 5 min at room temperature. After blocking with 2% BSA/PBS, cells were stained with anti-Myosin (Skeletal, Fast; Sigma) at 1:1000 dilution

overnight at 4°C. After washing with PBS, cells were incubated with Alexa Fluor® 647-labeled secondary antibody (Invitrogen) at 1:400 for 1 hr at room temperature, stained with Hoechst 33342 (1 µg/mL; Invitrogen) for 2 min at room temperature, washed and then mounted with ProLong Gold (Invitrogen). Microscopy was performed using the Axio Imager 2 with Apotome (Carl Zeiss) and AxioVision Software for analysis.

To quantitate *in vitro* myoblast fusion, the fusion index was determined as described previously¹⁵. Briefly, fluorescent images of six random fields were captured for each sample per experiment. ImageJ Cell Counter plugin software was used to quantitate nuclei number. The fusion index (the percentage of nuclei within myosin positive cells versus the total number of nuclei) was calculated for each field. Fusion indices from each field per sample were compiled and are depicted as the mean + the standard deviation (s.d.). In addition, the number of myosin positive myotubes per field with 2-4 nuclei (small myotubes) and 5 or greater nuclei (large myotubes) were recorded as another means to quantify myoblast fusion.

Flow cytometric analysis for apoptosis

To measure PtdSer exposure, floating and adherent C2C12 myoblasts or thymocytes were stained with APC-conjugated annexin V diluted 1:20 in the annexin V-binding buffer (eBioscience) for 10 min at room temperature. Cells were washed, resuspended in annexin V-binding buffer and assessed by flow cytometry. To measure selective membrane permeability during apoptosis, C2C12 cultures at the indicated time points after addition of fusion medium were treated with TO-PRO-3 (1µM; Molecular Probes) for 20 min at 37°C. Cells were washed in PBS, resuspended in PBS/0.5% BSA and assessed by flow cytometry. To measure caspase-3 activation, floating and adherent C2C12 myoblasts were fixed and permeabilized with Cytofix/Cytoperm solution (BD Biosciences) and stained with Alexa Fluor® 488-conjugated Cleaved Caspase-3 antibody diluted 1:20 in Cytoperm solution (Cell Signaling) for 20 min on ice. Cells were washed in Cytoperm solution, resuspended in PBS/0.5% BSA and assessed by flow cytometry.

Rescue of myoblast fusion

C2C12 cells were grown to 80% confluence in 15-cm tissue culture plates, after which they were induced to undergo myogenic differentiation as described previously. After 24 hours in fusion medium, the floating/dying myoblasts were collected at 1000 rpm for 5 minutes and resuspended gently into fresh fusion medium or growth medium. Unless specified otherwise, dying C2C12 myoblasts were added at a 1:1 ratio to plated, viable myoblasts at the time of the initial switch to fusion medium, or the myoblasts were <80% confluent if maintained in growth medium. The apoptotic myoblasts were spun down onto the viable myoblasts for 2 min at 500 rpm. This treatment was repeated each following day for 3 days total. Where indicated, dying myoblasts were pre-treated with GST-tagged BAI1 TSR (100 µg/mL) for 1 hour at 37°C before adding them to fusing cultures.

Thymuses were isolated from 4-5 week old mice and crushed through a 70 µm strainer to achieve single cell suspensions. Thymocytes were induced to undergo apoptosis by anti-Fas antibody treatment as described previously¹⁹. Briefly, 10×10⁶ thymocytes were collected and resuspended in C2C12 fusion medium with Protein-G (2 µg/mL; Sigma) and anti-CD95

(Fas) antibody (5 µg/mL; BD Biosciences). Two hours after treatment with anti-Fas, 5×10⁶ apoptotic thymocytes were added to confluent, zVAD treated C2C12 myoblasts and spun down for 2 min at 500 rpm. This treatment was repeated each following day for 3 days total.

Jurkat T cells (E6.1) were induced to undergo apoptosis by UV irradiation as described previously¹⁹. Briefly, Jurkat cells were collected at 1000 rpm for 5 minutes, resuspended in C2C12 growth medium and irradiated with 1500 mJoules of UV. Four hours after irradiation (recovery period), 4×10⁶ UV-treated or viable Jurkat cells were added to <80% confluent plated, viable C2C12 myoblasts and spun down for 2 min at 500 rpm. This treatment was repeated each following day for 3 days total.

Immunoblotting

C2C12 myoblasts were induced to fuse as described above and were collected at indicated time points after switch to fusion medium. Cells were lysed and total protein was quantified for each sample lysate using the D_c Protein Assay (Bio-Rad). Samples were analyzed by SDS-PAGE and immunoblotted. To detect BAI1 expression, a custom polyclonal rabbit antisera against a conserved C-terminal epitope was generated by injecting rabbits with a KLH-linked peptide (Novus Biologicals). Antibodies were used after one round of affinity purification on peptide columns. Peptide competition experiments and immunoblotting demonstrating antibody specificity were previously reported³¹. BAI1 antibody was used at a concentration of 1 µg/mL in 5% milk/TBS-T for immunoblotting in these studies.

Processing and immunostaining of mouse embryonic tissue

C57/BL6 mice were obtained from the Jackson Laboratories (Bar Harbor, ME). All animal procedures were performed as per protocols approved by the University of Virginia Animal Care and Use Committee.

For the detection of BAI1 in vivo, embryonic day (E) 14.5 mouse tissues were fixed by immersion in 4% paraformaldehyde in PBS and processed into paraffin blocks. 5 µm sections were processed for immunohistochemistry using standard techniques. Immunoperoxidase detection was performed using the ImPress polymeric peroxidase reagent (Vector), according to the supplier's instructions. The chromogen used was diaminobenzidine (Dako S3000) 1 mg/ml in PBS plus 0.02% hydrogen peroxide applied for 5 min and sections were counterstained with hematoxylin.

For the detection of apoptotic cells in vivo, embryos were harvested in PBS and postfixed in 4% paraformaldehyde in PBS for 24 hours at 4°C. Whole embryos were processed for paraffin infiltration by standard methods. Immunohistochemistry was performed on 8 µm thick paraffin sections using standard techniques. Primary antibodies utilized were: rabbit polyclonal anti-cleaved caspase 3 (1:100, Cell Signaling Technology), mouse monoclonal anti-actin (1:100, Sigma-Aldrich, clone AC-15). Immunofluorescence detection was performed using Alexa Fluor® 488 and Alexa Fluor® 546-conjugated secondary antibodies, diluted 1:2000 (Invitrogen, Carlsbad, CA). Images were acquired with an Olympus BX40 upright microscope and a Scion Firewire CCD camera (Scion, Frederick, MD). The entire paraspinal muscles of four sample sections were analyzed for presence of cleaved caspase 3+ bodies.

Stable transfections

For the generation of BAI1-GFP myoblasts, low-passage C2C12 myoblasts grown to 20-40% confluency in a 6-well dish were transfected with 20 µg of plasmid (pEBB-BAI1-GFP) + 5 µg of selection plasmid (pA-Puro) or selection plasmid alone using Lipofectamine 2000 (Invitrogen). Two days after transfection, the wells were replated into 10 cm² tissue culture plates and puromycin dihydrochloride (5 µg/mL; Sigma Aldrich) was added to cultures. GFP-positive/puromycin-resistant, or puromycin-resistant only control single-colony clones were isolated. Clones were analyzed for BAI1-GFP expression via flow cytometry and epifluorescence microscopy.

For the generation of ELMO2-knockdown shRNA, a 19-mer target sequence was identified using Dharmacon siDESIGN Center (AGC GCA AGG CCA TGT ATA C), and antisense oligos were generated using the pSicoOligomaker 1.5 program. The oligos were annealed and ligated into the pSicoR-GFP plasmid (Addgene), which co-expresses GFP for detection of expression. Low-passage C2C12 myoblasts grown to 30-40% confluency in a 6-well dish were transfected with 4 µg of ELMO2 or control shRNA plasmid along with 1 µg of selection plasmid (pA-Puro) using Lipofectamine 2000 (Invitrogen). The next day, the cells were replated into 10 cm² tissue culture plates and puromycin (5 µg/mL; Sigma) was added to cultures. The puromycin-resistant cells were maintained as a heterogenous population. To achieve a pure culture of ELMO2 or control shRNA-expressing myoblasts, the populations were electronically cell-sorted on the basis of GFP expression using an iCyt Reflection Cell Sorter (Sony Biotechnology Inc).

Lentiviral-mediated transduction

High-titer lentivirus containing wild-type human BAI1, a mutant BAI1-AAA or empty vector cDNA was generated using ViraPower HiPerform Lentiviral Expression system (Invitrogen) with several modifications. The *attB* sites and *lacZ* in pLenti6.3/V5-GW/*lacZ* were replaced with a multi-cloning site, and wild type or mutant BAI1 cDNA was inserted. In place of 293FT cells, lentivirus was produced in Lenti-X 293T cells (Clontech) transfected via CaCl₂ (Promega), and supernatants containing live virus were concentrated with Lenti-X Concentrator (Clontech) to better achieve high titer virus. Supernatants collected from two 10 cm² plates of virus-producing Lenti-X cells over 3 days were concentrated and applied to one 6 cm² dish of low-passage C2C12 myoblasts with polybrene (10 µg/mL; Sigma Aldrich). Growth medium was replaced every 24 hours with the addition of blasticidin (2.5µg/mL; Invitrogen) to growth medium 48 hours post-transduction. Transduced myoblasts were maintained as heterogeneous populations (no clones selected), and blasticidin selection was complete after 10 days. To specifically detect human BAI1 (wild-type or mutant), we measured expression via quantitative RT-PCR using a human-specific BAI1 TaqMan® probe (Hs00181777_m1) that did not cross react with the mouse endogenous BAI1 from C2C12 myoblasts. We performed rescue of myoblast fusion with these cells. Since apoptotic myoblasts taken from control or BAI1-overexpressing myoblast cultures had a similar effect in the rescue of zVAD-inhibited myoblast fusion, this established that BAI1 signaling within the healthy myoblasts rather than the dying myoblasts was more important in promoting fusion.

Quantitative RT-PCR

For the determination of *Elmo1*, *Elmo2* and *Elmo3* in C2C12 myoblasts and the determination of *myogenin* (*MyoG*) mRNA in fusing C2C12 myoblasts, DNAase I-treated total RNA was isolated using RNeasy kit (Qiagen). Superscript III SuperMix (Invitrogen), the provided random hexamer oligo, and 0.5 µg of total RNA as template were used to generate cDNA. qPCR was performed using gene-specific TaqMan® probes on a StepOne Plus Real-Time PCR instrument (Applied Biosystems). TaqMan® probes used are as follows: mouse *Elmo1* (Mm00519109_m1), mouse *Elmo2* (Mm01248046_m1), mouse *Elmo3* (Mm00555221_m1), mouse *MyoG* (Mm00446194_m1) and mouse *hprt* (Mm00446968_m1). For determination of *Bai1*, *Bai2* and *Bai3* mRNA in mouse muscle, total RNA was isolated from the tibialis anterior muscle of 5 individual mice using TriPure® kit (Roche Molecular Biochemicals) as previously described²². Superscript III SuperMix (Invitrogen), the provided random hexamer oligo, and 2 µg of total RNA as template were used to generate cDNA. qPCR was performed using gene-specific TaqMan® probes on a StepOne Plus Real-Time PCR instrument. TaqMan® probes used are as follows: mouse *Bai1* (Mm00558144_m1), mouse *Bai2* (Mm00557365_m1), mouse *Bai3* (Mm00657451_m1) and mouse *hprt* (same as above).

Mice

Embryonic stem cells carrying the exon trap mutation of *Bai1* locus (specifically losing exon 2 coding sequence) was purchased from Texas Institutes of Genomic Medicine. These ES cells (originally in the 129/Sv background) were used to generate chimeric mice via blastocyst injections. The chimeric progeny were crossed to C57Bl/6 and progeny between 2nd and 4th backcrosses were used in these studies. Tibialis anterior muscles from 12 week-old mice of the *Bai1*^{-/-} genotype, along with appropriate control littermates (gender matched), were used in the analysis as detailed below.

Muscle injury model

All animal procedures were approved by the University of Virginia Animal Care and Use Committee. Muscle injury was performed as previously described²². Briefly, 0.1 mL Cardiotoxin (*Naja nigricollis*) (0.071 mg/mL; Calbiochem) was injected into the left tibialis anterior (TA) muscles of 12-week-old *Bai1*^{-/-} and control littermate mice, and 0.1 mL saline was injected into the right TA muscle for control injury. The TA muscles were harvested at 14 days after injection and processed and analyzed as detailed below.

In vivo myofiber analysis

The tibialis anterior muscles of *Bai1*^{-/-} and control littermate mice were dissected and fixed by immersion in 4% paraformaldehyde in PBS and processed into paraffin blocks. 5 µm sections were processed for immunohistochemistry using standard techniques. Sections were stained with hematoxylin and eosin (H&E) and at least five fields were captured for each mouse section using the Axiovert 40 CFL (Carl Zeiss) and AxioVision Software for analysis. The cross sectional area (CSA) of each myofiber per field was quantitated using Cell Profiler²¹; output files were then screened for accuracy (to exclude mis-identified tubes) in a blinded fashion.

To quantitate myofiber fusion after injury, the *in vivo* fusion index was determined as described previously²³. Briefly, at least five fields of H&E stained myofiber cross-sections were captured for each mouse as above. ImageJ Cell Counter plugin software was used to quantitate the number of myofibers with single or multiple central nuclei. The *in vivo* fusion index (the percentage of TA myofibers containing multiple central nuclei versus the total number of myofibers) was calculated for each field. Fusion indices from each field per mouse were compiled and are depicted as the mean + the standard error of the mean (s.e.m.).

Myoblast engulfment assay

To determine the phagocytic capacity of myoblasts, four 15 cm² plates of C2C12 cells were serum-starved for 72 hours to induce apoptosis. The floating and adherent cells were collected and stained with TAMRA-SE (25 μM; Invitrogen). Next, 5×10⁵ TAMRA-SE stained dying myoblasts were added to viable, CFDA-SE (7.2 μM; Invitrogen) stained C2C12 cells on 2-chamber LabTek II Permanox chamber slides (Nunc) seeded 24 hours before at a density of 5×10⁴ cells per chamber. The two C2C12 populations were incubated together for 5 hours at 8.5% CO₂ 37°C, after which they were washed with PBS, fixed with 4% paraformaldehyde in PBS for 20 min at room temperature, stained with Hoechst 33342 (1 μg/mL; Invitrogen) for 2 min at room temperature and then washed and mounted with ProLong Gold (Invitrogen). Microscopy was performed using the Axio Imager 2 with Apotome (Carl Zeiss) and AxioVision software to analyze Z-stack images for three-dimensional analysis.

Analysis of apoptotic cell-contact during myoblast fusion

C2C12 cells were plated in growth medium on 2-chamber LabTek II Permanox chamber slides (Nunc) at 1×10⁵ cells/well and were induced to undergo myogenic differentiation as described with or without 100 μM zVAD-fmk. Fixable Viability Dye eFluor® 660 (1 μL/mL; eBioscience) was added to the fusion medium, for the course of the experiment, to label the myoblasts undergoing fusion medium-induced death. After 3 days, the myoblasts/myotubes were washed and fixed with 4% paraformaldehyde in PBS for 20 min at room temperature and permeabilized in 0.2% Triton X-100, 0.1% citrate in PBS for 5 min at room temperature. After blocking with 2% BSA/PBS, cells were stained with anti-Myosin (Skeletal, Fast; Sigma) at 1:1000 overnight at 4°C. After washing with PBS, cells were incubated with Alexa Fluor 488-labeled secondary antibody (Invitrogen) at 1:400 for 1 hr at room temperature, stained with Hoechst 33342 (1 μg/mL; Invitrogen) for 2 min at room temperature, washed and mounted with ProLong Gold (Invitrogen)..

To analyze the effect of apoptotic cells on the actin cytoskeleton of fusing myoblasts in a time course, C2C12 cells were plated in growth medium on 2-chamber LabTek II Permanox chamber slides (Nunc) at 1×10⁵ cells/well and were induced to undergo differentiation. Fixable Viability Dye eFluor® 660 (1 μL/mL; eBioscience) was added to the fusion medium during the course of the experiment to label the myoblasts undergoing death as part of the fusion process. For a total of 3 days, at 24hour intervals, a slide containing myoblasts/myotubes was washed and fixed with 4% paraformaldehyde in PBS for 20 min at room temperature and then stored at 4°C in 1%BSA in PBS until the conclusion of the time course. After the fixation of the last time point, all slides were permeabilized in 0.2% Triton

X-100, 0.1% citrate in PBS for 5 min at room temperature and then blocked with 2% BSA/PBS. Each slide was stained with 0.5 mL of Alexa Fluor® 555 Phalloidin (0.005 units/ μ L; Life Technologies) in 1%BSA in PBS for 20 min at room temperature, Hoechst 33342 (1 μ g/mL; Invitrogen) for 2 min at room temperature, then washed and mounted with ProLong Gold (Invitrogen). Microscopy was performed using the Axio Imager 2 with Apotome (Carl Zeiss) and AxioVision Software for analysis.

Time-lapse microscopy of myoblast fusion

C2C12 myoblasts were plated on Poly-L-Lysine (Sigma) coated glass coverslips. Once 80-100% cell confluency was achieved, coverslips were inserted into a POC-R2 chamber (Pecon) and fusion medium pre-equilibrated with 8.5% CO₂ including 1 μ M TO-PRO-3 was added. Time-lapse images were captured every 20 minutes for 72 hours on a 37 degree-heated stage using the Axio Imager 2 with Apotome (Carl Zeiss) and AxioVision Software for analysis.

Statistical analysis

Unless otherwise described, the data are representative of at least three independent experiments and are shown as mean \pm the standard deviation (s.d.). For analysis of statistical difference between two groups, a Student's two-tailed unpaired *t*-test was applied. For analysis of statistical difference between three or more groups, a one-way ANOVA with Bonferroni's multiple comparison test was applied. Significance was defined when *P* values were <0.05.

Supplementary Material

Refer to Web version on PubMed Central for supplementary material.

Acknowledgments

We thank members of the Ravichandran laboratory for their valuable suggestions at many stages of this work. We also thank L. Haney, A. Bruce and A. Dutta for technical suggestions and assistance and M. Hufford and A. Fond for help with statistical analysis. We thank members of the University of Virginia Flow Cytometry Core, Research Histology Core and Gene Targeting and Transgenic Facility for cell sorting, histological services and transgenic mouse generation. This work was supported by a grant from the NIGMS/NIH and the Center for Cell Clearance at the University of Virginia.

References

1. Abmayr SM, Pavlath GK. Myoblast fusion: lessons from flies and mice. *Development*. 2012; 139:641–656.10.1242/dev.068353 [PubMed: 22274696]
2. Chen EH, Olson EN. Towards a molecular pathway for myoblast fusion in *Drosophila*. *Trends Cell Biol*. 2004; 14:452–460.10.1016/j.tcb.2004.07.008 [PubMed: 15308212]
3. Park D, et al. BAI1 is an engulfment receptor for apoptotic cells upstream of the ELMO/Dock180/Rac module. *Nature*. 2007; 450:430–434.10.1038/nature06329 [PubMed: 17960134]
4. Gumienny TL, et al. CED-12/ELMO, a novel member of the CrkII/Dock180/Rac pathway, is required for phagocytosis and cell migration. *Cell*. 2001; 107:27–41. [PubMed: 11595183]
5. Hasegawa H, et al. DOCK180, a major CRK-binding protein, alters cell morphology upon translocation to the cell membrane. *Molecular and cellular biology*. 1996; 16:1770–1776. [PubMed: 8657152]

6. Brugnera E, et al. Unconventional Rac-GEF activity is mediated through the Dock180-ELMO complex. *Nat Cell Biol.* 2002; 4:574–582.10.1038/ncb824 [PubMed: 12134158]
7. Erickson MR, Galletta BJ, Abmayr SM. Drosophila myoblast city encodes a conserved protein that is essential for myoblast fusion, dorsal closure, and cytoskeletal organization. *The Journal of cell biology.* 1997; 138:589–603. [PubMed: 9245788]
8. Hakeda-Suzuki S, et al. Rac function and regulation during Drosophila development. *Nature.* 2002; 416:438–442.10.1038/416438a [PubMed: 11919634]
9. Moore CA, Parkin CA, Bidet Y, Ingham PW. A role for the Myoblast city homologues Dock1 and Dock5 and the adaptor proteins Crk and Crk-like in zebrafish myoblast fusion. *Development.* 2007; 134:3145–3153.10.1242/dev.001214 [PubMed: 17670792]
10. Laurin M, et al. The atypical Rac activator Dock180 (Dock1) regulates myoblast fusion in vivo. *Proceedings of the National Academy of Sciences of the United States of America.* 2008; 105:15446–15451.10.1073/pnas.0805546105 [PubMed: 18820033]
11. Vasyutina E, Martarelli B, Brakebusch C, Wende H, Birchmeier C. The small G-proteins Rac1 and Cdc42 are essential for myoblast fusion in the mouse. *Proceedings of the National Academy of Sciences of the United States of America.* 2009; 106:8935–8940.10.1073/pnas.0902501106 [PubMed: 19443691]
12. Geisbrecht ER, et al. Drosophila ELMO/CED-12 interacts with Myoblast city to direct myoblast fusion and ommatidial organization. *Dev Biol.* 2008; 314:137–149.10.1016/j.ydbio.2007.11.022 [PubMed: 18163987]
13. Yaffe D, Saxel O. Serial passaging and differentiation of myogenic cells isolated from dystrophic mouse muscle. *Nature.* 1977; 270:725–727. [PubMed: 563524]
14. Cornelison DD. Context matters: in vivo and in vitro influences on muscle satellite cell activity. *Journal of cellular biochemistry.* 2008; 105:663–669.10.1002/jcb.21892 [PubMed: 18759329]
15. Pajcini KV, Pomerantz JH, Alkan O, Doyonnas R, Blau HM. Myoblasts and macrophages share molecular components that contribute to cell-cell fusion. *The Journal of cell biology.* 2008; 180:1005–1019.10.1083/jcb.200707191 [PubMed: 18332221]
16. Shutes A, et al. Specificity and mechanism of action of EHT 1864, a novel small molecule inhibitor of Rac family small GTPases. *J Biol Chem.* 2007; 282:35666–35678.10.1074/jbc.M703571200 [PubMed: 17932039]
17. van den Eijnde SM, et al. Transient expression of phosphatidylserine at cell-cell contact areas is required for myotube formation. *J Cell Sci.* 2001; 114:3631–3642. [PubMed: 11707515]
18. Jeong J, Conboy IM. Phosphatidylserine directly and positively regulates fusion of myoblasts into myotubes. *Biochem Biophys Res Commun.* 2011; 414:9–13.10.1016/j.bbrc.2011.08.128 [PubMed: 21910971]
19. Chekeni FB, et al. Pannexin 1 channels mediate ‘find-me’ signal release and membrane permeability during apoptosis. *Nature.* 2010; 467:863–867.10.1038/nature09413 [PubMed: 20944749]
20. Hasty P, et al. Muscle deficiency and neonatal death in mice with a targeted mutation in the myogenin gene. *Nature.* 1993; 364:501–506.10.1038/364501a0 [PubMed: 8393145]
21. Kametsky L, et al. Improved structure, function and compatibility for CellProfiler: modular high-throughput image analysis software. *Bioinformatics.* 2011; 27:1179–1180.10.1093/bioinformatics/btr095 [PubMed: 21349861]
22. Yan Z, et al. Highly coordinated gene regulation in mouse skeletal muscle regeneration. *J Biol Chem.* 2003; 278:8826–8836.10.1074/jbc.M209879200 [PubMed: 12477723]
23. Grounds MD, Radley HG, Lynch GS, Nagaraju K, De Luca A. Towards developing standard operating procedures for pre-clinical testing in the mdx mouse model of Duchenne muscular dystrophy. *Neurobiol Dis.* 2008; 31:1–19.10.1016/j.nbd.2008.03.008 [PubMed: 18499465]
24. Chen YW, Zhao P, Borup R, Hoffman EP. Expression profiling in the muscular dystrophies: identification of novel aspects of molecular pathophysiology. *J Cell Biol.* 2000; 151:1321–1336. [PubMed: 11121445]
25. Haslett JN, et al. Gene expression comparison of biopsies from Duchenne muscular dystrophy (DMD) and normal skeletal muscle. *Proc Natl Acad Sci U S A.* 2002; 99:15000–15005.10.1073/pnas.192571199 [PubMed: 12415109]

26. Bakay M, et al. Nuclear envelope dystrophies show a transcriptional fingerprint suggesting disruption of Rb-MyoD pathways in muscle regeneration. *Brain*. 2006; 129:996–1013.10.1093/brain/awl023 [PubMed: 16478798]
27. Bialek P, et al. Distinct protein degradation profiles are induced by different disuse models of skeletal muscle atrophy. *Physiol Genomics*. 2011; 43:1075–1086.10.1152/physiolgenomics.00247.2010 [PubMed: 21791639]
28. Sens KL, et al. An invasive podosome-like structure promotes fusion pore formation during myoblast fusion. *J Cell Biol*. 2010; 191:1013–1027.10.1083/jcb.201006006 [PubMed: 21098115]
29. Phaneuf S, Leeuwenburgh C. Apoptosis and exercise. *Med Sci Sports Exerc*. 2001; 33:393–396. [PubMed: 11252065]
30. Ravichandran KS. Find-me and eat-me signals in apoptotic cell clearance: progress and conundrums. *J Exp Med*. 2010; 207:1807–1817.10.1084/jem.20101157 [PubMed: 20805564]
31. Sokolowski JD, et al. Brain-specific angiogenesis inhibitor-1 expression in astrocytes and neurons: implications for its dual function as an apoptotic engulfment receptor. *Brain, behavior, and immunity*. 2011; 25:915–921.10.1016/j.bbi.2010.09.021

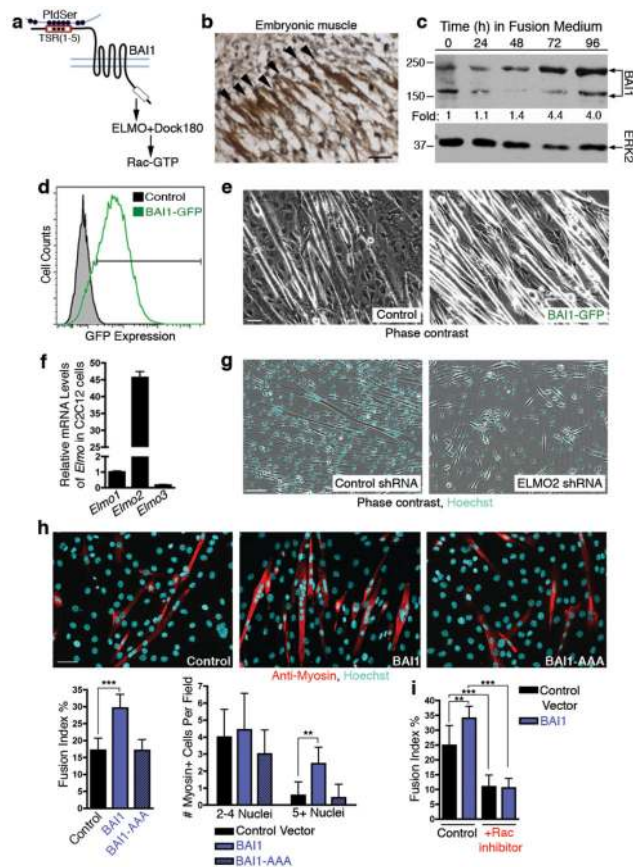


Figure 1. The phosphatidyserine receptor BAI1 promotes myoblast fusion
a, Schematic of BAI1 depicting TSR repeats that bind PtdSer on apoptotic cells and the ELMO1-binding site in its cytoplasmic tail. **b**, Endogenous BAI1 protein detected (brown) within developing E14.5 mouse paraspinal muscle. **c**, BAI1 protein expression in fusing C2C12 myoblast cultures (170-kDa monomer and 220-kDa dimer³). **d**, BAI1-GFP expression in stable C2C12 clones analyzed by flow cytometry. **e**, Myoblast fusion in control or BAI1-GFP stable clones. **f**, qPCR analysis of *Elmo1*, *Elmo2* and *Elmo3* mRNA (normalized to *HPRT*) in C2C12 myoblasts (expression compared to *Elmo1*). **g**, Fewer myotubes and fewer nuclei within myotubes of ELMO2 shRNA stable cells. Scale bars= 100 μ m. **h**, Myoblast fusion in C2C12 cultures transduced with lentivirus encoding wild type BAI1, mutant BAI1-AAA, or control vector. For determining fusion index (see methods), nuclei (Hoechst, cyan) and myotubes (anti-Myosin antibody, red) were labeled, and six fields analyzed per sample for each experiment (** P <0.001, ** P <0.01). **i**, BAI1-mediated increased myoblast fusion is blocked by Rac inhibitor (EHT1864) (** P <0.01, *** P <0.001). All data represent at least three independent experiments. Error bars indicate s.d., and scale bars= 50 μ m unless otherwise stated.

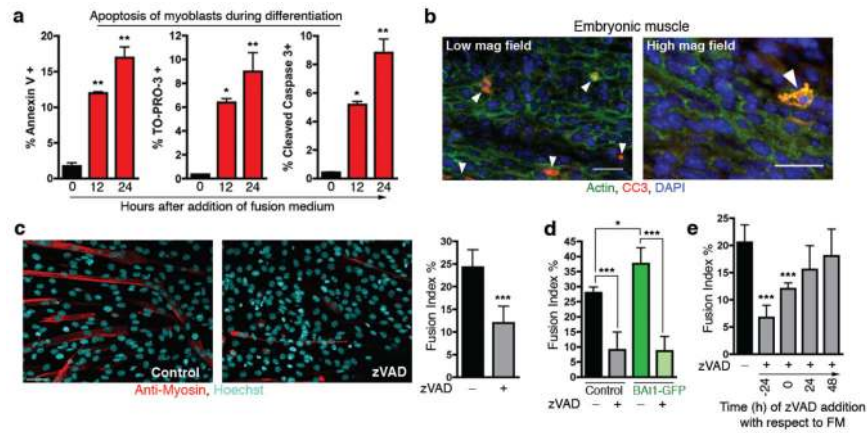


Figure 2. Apoptosis of myoblasts is necessary for fusion

a, Apoptosis of C2C12 myoblasts at indicated time-points during fusion was assessed by Annexin V, TO-PRO-3 (permeable to apoptotic cells), or anti-cleaved caspase 3 (CC3) after permeabilization ($*P<0.05$, $**P<0.01$). **b**, Dying cells (white arrowheads) were detected in developing E14.5 mouse skeletal muscle tissue with CC3 antibody (red); striated muscle fibers detected with anti-actin (green). Higher magnification image displays characteristic blebbing of CC3-positive apoptotic cells. Scale bars= 25 μ m. **c**, C2C12 cultures were treated with the pan-caspase inhibitor zVAD and analyzed for nuclei (Hoechst, cyan), myotubes (anti-Myosin, red). Six fields were analyzed per treatment for each experiment ($***P=0.0002$). **e**, BAI1-mediated enhancement of myoblast fusion is also blocked by zVAD ($*P<0.05$, $***P<0.001$). **f**, Myoblast fusion is inhibited by zVAD, only if added before cell death occurs ($***P<0.001$). All data represent at least three independent experiments. Error bars indicate s.d., and scale bars= 50 μ m unless otherwise stated.

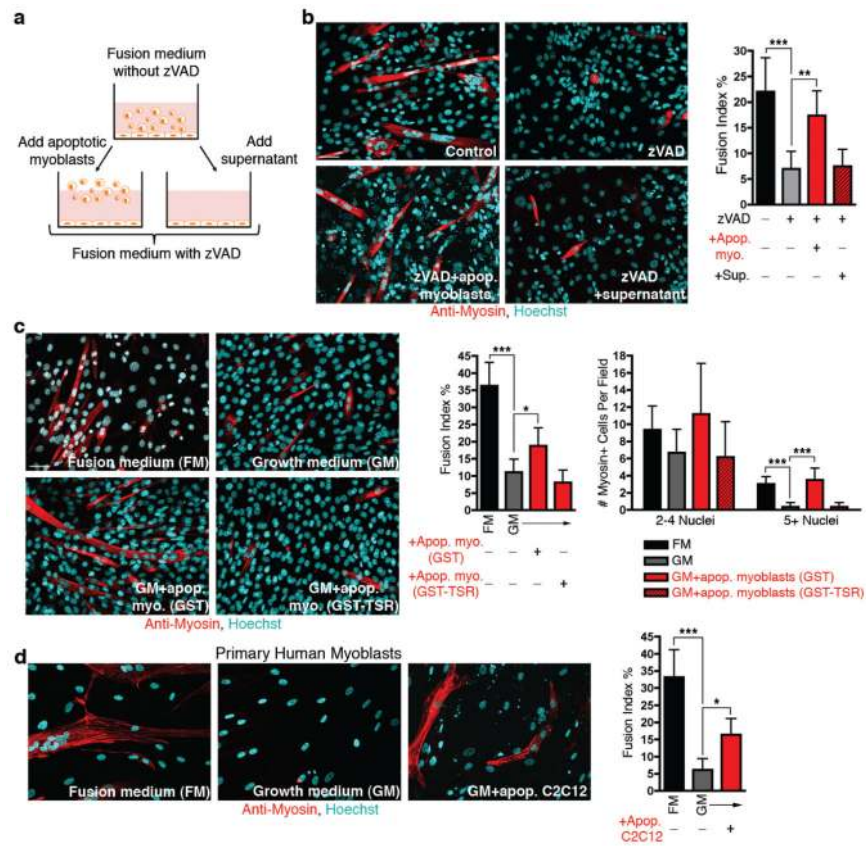


Figure 3. Cell-cell contact via apoptotic myoblasts promotes myoblast fusion

a, Schematic depicting add-back of apoptotic myoblasts. **b**, Apoptotic myoblasts or cell-free supernatants were added to C2C12 cells treated with zVAD in fusion medium. Nuclei (Hoechst, cyan) and myotubes (anti-Myosin antibody, red) were labeled, and six fields analyzed per treatment group for each experiment ($***P < 0.001$). **c**, C2C12 cultures were maintained in fusion medium (FM), growth medium (GM), or GM+apoptotic C2C12 cells pre-incubated with either control GST protein or GST-TSR (to mask PtdSer) and analyzed as above ($*P < 0.05$, $***P < 0.001$). Note the increase in myotubes with ≥ 5 nuclei (large myotubes) ($***P < 0.001$). **d**, Human primary skeletal myoblast cultures were maintained in fusion medium (FM), growth medium (GM), or GM with apoptotic C2C12 myoblasts and analyzed as above ($*P < 0.05$, $***P < 0.001$). All data represent at least three independent experiments. Error bars indicate s.d., and scale bars = 50 μm .

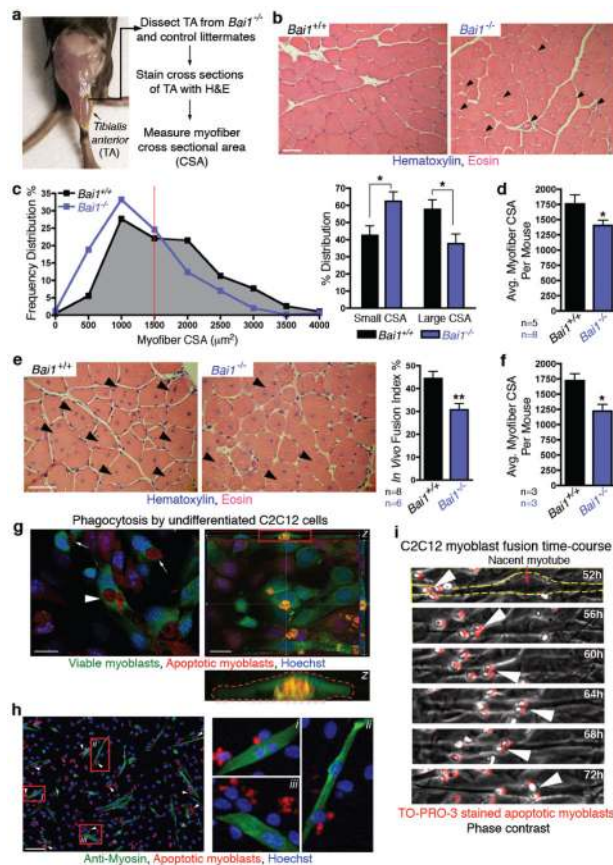


Figure 4. Defective development of myofibers in *Bai1*-null mice

a, Schematic of TA muscle analysis. **b**, TA muscles from *Bai1*^{-/-} mice display smaller myofibers (by H&E staining). Arrowheads show smaller myofibers in the *Bai1*^{-/-} mice. **c**, The percent distribution of myofibers by CSA (µm²), with the redline demarcating ‘small’ and ‘large’ myofibers based on CSA of 1500µm²; the distribution of small and large myofibers is shown on right. **d**, Average myofiber area (in µm²) per mouse (**P*<0.05; n=5 or n=8 male mice for *Bai1*^{+/+} and *Bai1*^{-/-}, respectively). **e**, Regenerated TA muscles from *Bai1*-null mice (14 days after cardiotoxin-induced injury) show fewer regenerating myofibers with central nuclei (arrowhead). (right) *In vivo* fusion index for regenerating myofibers in control and *Bai1*-null mice (see methods) (***P*<0.01; n=8 mice for *Bai1*^{+/+} and n=6 mice for *Bai1*^{-/-}). **f**, Regenerated *Bai1*-null myofibers display smaller average myofiber area (in µm²) per mouse (**P*<0.05; n=3 male mice each for *Bai1*^{+/+} and *Bai1*^{-/-}). **e**, **f** are representative of two independent injury experiments. **g**, (Left) Image of viable myoblasts (green) engulfing apoptotic myoblasts (red). Arrowheads, engulfed cells; arrows, phagocytic cups around partially engulfed targets. The magnified z dimension within the red box (bottom), outlines the green signal from the viable myoblast completely surrounding the orange dying target. Scale bars= 20µm. **i**, Time-lapse images monitoring apoptotic myoblasts becoming TO-PRO-3 labeled (red) as they emerge. See Supplementary Fig. 6 and Supplementary movie SM1 for additional frames. **j**, Apoptotic myoblasts (Viability Dye, red) are often in proximity but not within the fusing myoblasts or myotubes (Anti-myosin, green). Nuclei are stained blue (Hoechst). Red boxes are shown in higher magnification

(right). Scale bar= 100 μ m. Error bars indicate s.e.m., and scale bars= 50 μ m, unless otherwise indicated.

Author Manuscript

Author Manuscript

Author Manuscript

Author Manuscript